We are IntechOpen, the world's leading publisher of Open Access books Built by scientists, for scientists

5,000
Open access books available

125,000
International authors and editors

140M
Downloads

Our authors are among the

154
Countries delivered to

TOP 1%
most cited scientists

12.2%
Contributors from top 500 universities

WEB OF SCIENCE™

Selection of our books indexed in the Book Citation Index in Web of Science™ Core Collection (BKCI)

Interested in publishing with us?
Contact book.department@intechopen.com

Numbers displayed above are based on latest data collected.
For more information visit www.intechopen.com

Chapter

Comparative Evaluation of Hydrochars and Pyrochars for Phosphate Adsorption from Wastewater

Aicha Slassi Sennou, Shuangning Xiu and Abolghasem Shahbazi

Abstract

Biochar represents the rich carbon residues that remains after thermally pyrolyzing or liquefying different biomass types in an oxygen-free environment. The availability of animal and agricultural wastes makes the biochar a low-cost product. It is, as a carbon-rich product, resistant to mineralization and decomposition. Biochar can be used as a multifunctional material in many applications in the environmental and agricultural sectors. Recently, a growing interest for the use of biochar in different fields is rising because of its use as a sorbent for organic and nonorganic contaminants from aqueous solutions. In this chapter, recent studies on pyrochar/hydrochar production, characterization, and phosphate adsorption are reviewed and summarized. The remediation technologies for phosphate removal from contaminated water using biochar are also discussed. The effects of reaction temperature and initial solution pH on phosphate adsorption onto biochar are compared. In addition, we highlighted the models that are used for adsorption kinetics and adsorption isotherms.

Keywords: biochar, hydrochar, pyrochar, pyrolysis, hydrothermal carbonization, phosphate, filtration

1. Introduction

Phosphorus (P) is an essential nutrient for the growth of plants; however, its excessive release into runoff water can impose a danger on environmental health [1]. Phosphor soluble in water is present under three forms, ortho-, poly-, and organic phosphate. Orthophosphate comprises HPO_4^-, $H_2PO_4^{2-}$, H_3PO_4, and PO_4^{3-} which encourages the evolution of aquatic microorganisms and macroorganisms leading to eutrophication. Eutrophication is caused by the presence of excessive phosphate amounts and has adverse impacts on the water ecosystem. In fact, even low amounts of phosphate 0.02 mg/L can cause algae to grow leading to reduced oxygen in water that could kill fish and damage wildlife [2]. The municipal sewage phosphate concentration is in the 4–15 mg-P/L range, while it exceeds 10 mg-P/L in industrial wastewaters. Consequently, phosphate concentration from wastewater needs to be reduced prior to the discharge in water bodies. On the other hand,

phsophorus is a non-renewable source available in limited quantities in nature with Morocco owning approximately 75% of the market [3]. There is an uncertainty about the lifetime of the remaining reserves and their accessibility. Studies have shown that P reserves are limited and will deplete soon with the increasing use of phosphorus as a fertilizer for agronomic production. Thus, it is crucial to develop effective phosphate removal technologies from aqueous solution.

Many technologies have been studied for phosphate removal from industrial and municipal effluents; these have been categorized into chemical, physical, and biological wastewater treatments. Studies have proven the effectiveness of biological and chemical treatments. These treatment methods use plants such as algae or chemicals such as alum, lime, and ferric salts to remove phosphorus from water before discharge into water bodies. Studies have shown that 97% of the total phosphorus (TP) could be removed from aqueous solutions with the use of phosphate biological treatment methods which does not present the risk of adding chemical contaminants to the water. However, the phosphate removal efficiency may be low due to its sensitivity to operation conditions [1]. However, other treatment method costs remain expensive, and some of them necessitate continuous checking of the operating conditions in order to prevent the introduction of new contaminants into the water. Thus, developing a cost-effective technology to prevent eutrophication and manage phosphorus recovery will prevent the shortage of this important element as it can be recycled and reused if it is successfully recovered from wastewater.

Adsorption presents a low-cost and efficient method for phosphorus removal due to its cost-effectiveness, accessibility, and performance. However, the high cost of traditional adsorbents (e.g., active carbon and anion exchange resins) and the difficulty of disposal are problems that limit their use. Thus, researchers study the development possibility of low-cost adsorbents that could come from cheap and available products such as biomass. Biochar has been studied as a prospective adsorbent for its properties including low cost, availability, stability, high porosity, and non-costly preparation and upgrading [2]. However, powder carbon-based biochars were identified to be difficult to separate from aqueous solutions which requires the use of magnetic separation that requires the addition of magnetic iron oxide through chemical co-precipitation [4].

Biochar has many advantages over traditional adsorbents such as being environmentally friendly, recyclable, low cost, easy to prepare, and having a high porosity. Consequently, researchers have studied the potential application of biochar as a phosphate adsorbent from wastewater [5] and its use as a fertilizer for soil quality enhancement. However, non-modified biochar with a surface charged negatively has a limited adsorption capacity for anionic pollutants which requires impregnating some metals on the biochar surface (Fe, Mg, Al, etc.) [2]. The preparation process of magnetic adsorbents is considered complicated and costly due to the complicated steps involved starting by the precursor preparation, oxidation of activated carbon, and then iron grafting [6]. For this reason, biochar use as a phosphate adsorbent from wastewater needs to be examined. Factors affecting the effectiveness of the anionic pollutant adsorption such as the functional site amount, affinity, dispersion, and surface accessibility need to be considered [7]. Some researchers studied the phosphate adsorption capacity of modified biochar. Junk et al. prepared magnetic biochar by magnesium ferrite impregnation through co-precipitation of Mg and Fe and pyrolysis and found to have an adsorption capacity of 487.99 mg P/g where P is the symbol of phosphorus [8, 9]. Junk et al. adsorption rate is considered among the highest when compared to other biochars adsorption rates 41.16 mg P/g, 125.40 mg P/g, 135 mg P/g [13, 17, 40]; this is shown later in Section 4 [7].

Other techniques are also employed to improve biochar surface characteristics for better adsorption. These treatment methods can be divided into gas phase

and liquid phase. Gas phase uses steam or carbon dioxide for achieving physical activation, whereas liquid phase uses chemicals [10]. Both liquid phase and gas phase treatment methods use activation temperatures higher than 450°C. Chemical activation has advantages over physical activation due to its less cost and time along with higher char porosity [11].

2. Phosphate in water bodies

P is a vital nutrient for the growth of aquatic organisms, plants, and animals [12, 13]. It also plays an essential role as a limiting nutrient, preventing the development of algae and aquatic plants in the water ecosystem [14]. TP amount needs to be less than 0.03 mg/L, while phosphate level between 0.005 and 0.05 mg/L as an excessive amount of phosphate in water bodies causes eutrophication. Eutrophication leads to the destruction of water ecosystem including rivers, lakes, and seas causing harm to human health and an increase to the water treatment cost [15]. Natural phosphate reserves are limited and will be depleted in 50–100 years [16]. Thus, phosphorus recovery from phosphate-rich wastewater can simultaneously solve the phosphorus depletion issue and improve water quality [17].

3. Biochar production through pyrolysis and hydrothermal carbonization (HTC)

3.1 Biochar production from hydrothermal carbonization

Biomass HTC is performed at temperatures ranging from 160–800°C. It is categorized into low-temperature reactions (lower than 300°C) and high-temperature reactions (300–800°C). During high-temperature HTC, the principal reaction is gasification, and the products are gases including hydrogen and methane [18] while carbonization takes place at low temperatures. Gasification favors the production of methane and hydrogen through

$$C_6H_{12}O_6 + 6H_2O \rightarrow 6CO_2 + 12H_2 \quad (1)$$

$$C_6H_{12}O_6 \rightarrow 3CH_4 + 3CO_2 \quad (2)$$

Hydrogen formation is endothermic and methane formation is exothermic. Therefore, at high temperatures hydrogen formation exceeds methane as illustrated in **Figure 1**.

Hydrothermal carbonization is used for high moisture content biomass contrarily to pyrolysis and gasification that deals with low moisture content biomass [19]. Many factors affect the hydrochar characteristics. These include the water-to-biomass ratio, reaction temperature, residence time, and pressure. Hydrochar is defined as the product of HTC reaction and has a 40–70 wt% yield. Hydrochars have lower yields but high higher heating value (HHV) than low-temperature pyrolysis (LTP) pyrochars [20]. The ultimate analysis confirmed these findings as it shows hydrochars having high carbon contents and low oxygen contents than pyrochars. Pyrochars have higher yields than hydrochars and thus higher-energy yields despite their lower HHVs. This indicates that biomass experienced a deep carbonization and decomposition in the LTP process. Oliveira et al. [21] showed that deeper carbonization of biochar can be achieved by combining different

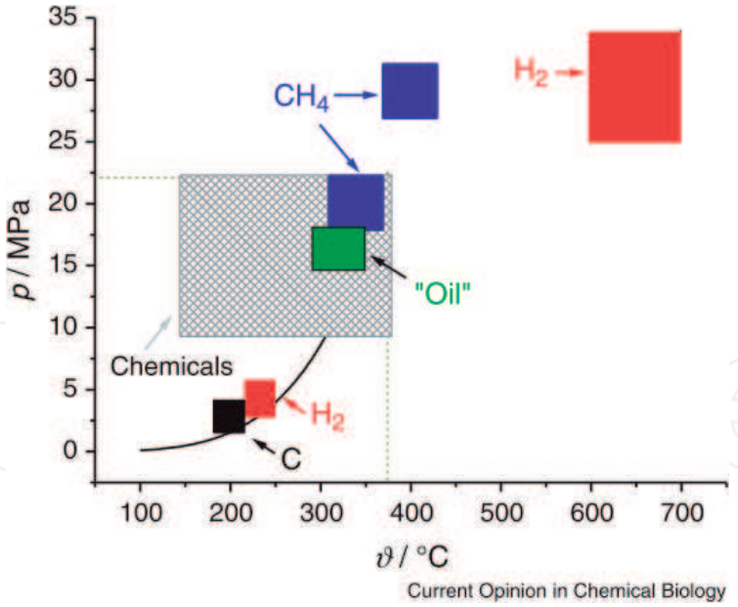

Figure 1.
Different biomass conversion processes overview and vapor-pressure water curve [18].

agricultural residues and different types of biomass. The use of lignocellulosic residues leads to hydrochars with high-energy yields.

In addition, hydrochars produced good dewatering and drying properties. The water involved in the process could be reused which will reduce the environmental impact and increase the energy efficiency. Different researchers have studied production conditions such as feedstock, temperature, and residence time on hydrochar. Sabio et al. [22] reported that the main factors affecting the hydrochar solid yield are residence time and temperature. Producing hydrochars in the ideal conditions can contribute to promote energy densification (increase in HHV).

3.2 Biochar production from biomass pyrolysis

Pyrolysis is used for the conversion of biomass into alternative products such as biochar, syngas, and bio-oil in an oxygen-free environment at temperatures ranging from 300 to 900°C. There are different types of reactors used to produce biochar including pyrolysis rotary drums, paddle pyrolysis kiln, and auger reactor [23].

The rotary drum reactor is considered a reliable system for biochar production. The reactor is composed of internal concentric steel tube and a rotary part made of insulated mantle. The mantle supports a sequence of radial steel fins and connects to the steel tube. Two fixed parts at the rotary end are responsible of the charge and the discharge of solid and gaseous products. The biomass moves through the carbonization kiln, passes inside the internal concentric tube, and is moved at increasing temperatures through various sections. The biomass temperature fumes enter the furnace and increase the temperature to 500°C. The carbonization process requires heat that is delivered by burning gases and pyrolysis vapors. The process is energy independent except the starting phase that uses external combustion. Fumes exit the reactor through the chimney while the produced biochar is gathered in a stocking silo [24] (**Figure 2**).

The auger pyrolysis reactor is normally nourished with wood waste by a hopper at the retort end. The wood waste is transported through an auger into other extremities for carbonization. The vapors and gases are sent to a condenser, and

the biochar is collected in the retort through a single tube. The main structure at the lowest level includes a combustion chamber where carbonization occurs. The combustion chamber uses gases to provide heat [24] (**Figure 3**).

The paddle pyrolysis reactor is a low-temperature gasifier. Its main characteristics is to move and mix biomass increasing the heat transfer on the material surface. The system output is biochar and syngas; the reactor has a unique cleanup system to produce syngas for downstream applications [24].

Pyrolysis can be divided into two types, slow and fast pyrolysis, based on the reaction conditions (heating rate, residence time, pressure, and mainly temperature) [25]. Slow pyrolysis is conducted in temperatures ranging from 400 to 600°C and is used in applications that seek a high biochar yield and a low bio-oil and syngas products including CH_4, H_2, CO, CO_2, and C1–C2 hydrocarbons. The reaction is conducted at atmospheric pressure and residence time longer than 1 h at a heating rate in the range of 5–7°C/min [25, 26]. These conditions lead to more cracking reactions which decrease the liquid yield and consequently increase biochar yield [27]. Slow pyrolysis also called conventional carbonization process produces high biochar yields mainly for feedstocks with high ash content, lignin, and particle size [28]. Another factor that can contribute to high biochar yield is the increasing particle size of the sample.

This is a simple, cost-effective but powerfully built process which is mainly applicable to small-scale biochar production farms. On the other hand, fast pyrolysis has more opportunities toward increasing bio-oil yield up to 75% from original

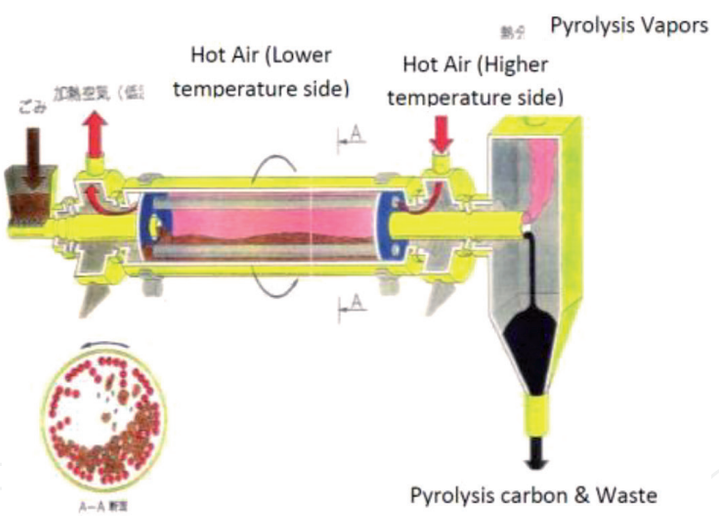

Figure 2.
Pyrolysis rotary drum [24].

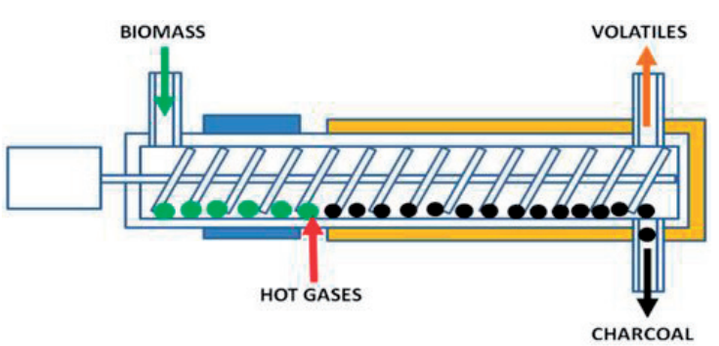

Figure 3.
Auger reactor [24].

raw biomass, and in contrast to slow pyrolysis the heating rate is higher than 200°C/min and residence time less than 10 s which favors the decrease in biochar yield [29].

4. Remediation technologies for phosphate removal in aqueous solutions using biochar

Many researchers have explored different paths for phosphate adsorption from wastewater. Methods have been studied including solvent extraction, chemical precipitation, gravity separation, ion exchange, reverse osmosis, solvent extraction, electrodialysis and electrocoagulation, adsorption, and flotation for phosphate removal from sewage system [30]. Adsorption is preferred for cost-effectiveness. However, waste sludge disposal resulting from adsorption of phosphate from wastewater is complicated and expensive which hinders the use of adsorption technique for phosphate removal in industrial scale.

The use of metal salts has been explored for phosphate removal. Most metals have a strong ability to adsorb contaminants using electrostatic attraction between the surface charged negatively and the metal ions charged positively [31]. Moreover, there is a limitation on transforming agricultural residues to green by-products since most farmers burn their crop stalk causing more greenhouse gas emissions and harm to the environment. Biochar could be used as a clean environmental by-product as it is produced in an oxygen-free environment and can be used for different applications [13]. The use of biochar and impregnation of metal oxides on its surface for phosphate adsorption was studied as a technique for contaminant removal.

Techniques for phosphorus recovery can be categorized as physical (electrodialysis, reverse osmosis, ion exchange) [1], chemical, and biological [32]. Some of the mostly used techniques are ion exchange, chemical precipitation, electrocoagulation, chemical precipitation, crystallization, and adsorption. Phosphorus chemical precipitation can be achieved by the deposition of some metal elements and metal oxides. Crystallization can be represented by attractive struvite (magnesium ammonium phosphate) which is a white crystal containing important elements for the growth of plants. Struvite is composed of Mg, P, and N with equal molar concentrations. Struvite can be crystallized and applied to the soil as a fertilizer or used for the recovery of phosphorus and nitrogen. However, the economic feasibility of struvite precipitation is influenced by the costs of reagents such as magnesium. Magnesium sources such as MgO are environmental materials; their advantage is the high alkalinity than other alkalis. Alkalinity plays an important role in acid neutralization as well as creation of adequate pH region for crystallization. The MgO available in the market is a solid mineral which releases low amounts of Mg due to slow dissolution [33]. Struvite crystallization can be used for sludge anaerobic digestion due to the high concentration of ammonia and phosphorus in reactors. Struvite formation formula is

$$Mg^{2+} + NH_4^+ + PO_4^{3-} + 6H_2O \rightarrow MgNH_4PO_4 6(H_2O) \quad (3)$$

The struvite chemical precipitation has high adsorption of soluble phosphate 80–90% [34]. Struvite precipitation faces challenges in phosphorus recovery from wastewater when the phosphorus concentration is below 50 mg/L and the suspended solid concentration is higher than 2000 mg/L [35]. Mariana et al. [35] suggested the application of struvite precipitation in secondary streams with high phosphorus concentrations.

Adsorption is another attractive technology. It has been well-known for its simplicity, low cost, and high adsorption capacity. Different adsorbents have been tested for phosphate adsorption from wastewater including activated carbon, metal-based materials, and designed engineering particles. These adsorbents have shown some drawbacks such as high cost and inefficiency. Thus, increasing interest is going to agricultural by-products. During the past several years, research studies have been done on the removal of contaminants from aqueous solutions using biochar. Biochar is considered a potential great adsorbent because of its high ion exchange capacity, large surface area, and abundant functional groups. However, adsorption of biochar to anion pollutants such as $PO4^{3-}$ phosphate anion is limited due to the negatively charged surface of biochar and its low anion exchange capacity. Thus, studies suggested that the removal capacity can be improved by using chemical co-precipitation to deposit metal element cations (Ca^{2+}, Fe^{3+}, Al^{3+}, Mg^{2+}) or metal oxides (CaO, MgO, La_2O_3, Fe_2O_3, Al_2O_3). Metal oxides and elements react with oxyanions such as PO_4^{3-}, resulting in improved anion removal rate [36].

Ion exchange is carried to remove certain ions from an aqueous solution. It is used for purification of aqueous solutions with the use of polymeric ion exchange resin or other materials that have ion exchange properties. Ion exchangers can be anion exchangers (exchanging ions charged negatively) or cation exchangers (exchanging ions charged positively). Ion exchange is considered a reversible process where the ion exchanger could be loaded with appropriate ions through washing with these ions excess. Electrostatic attraction is a force that binds particles to non-conducting surfaces. Simple Coulombic attraction helps in the attraction of charged particles to oppositely charged surfaces. However, both surfaces do not need to be charged as particles can be attracted to neutral surfaces [37].

Biochar has been produced from different precursors at different conditions and tested in the laboratory to study its adsorption capacity. In recent years, it has been noticed a growing interest in converting anaerobic digestion residue to biochar [38]. Jiwei et al. [9] produced a MgO-modified biochar using chemical co-precipitation of Mg^{2+} and Fe^{3+} on biochar from anaerobic digestion residue. The modified biochar was pyrolyzed at different temperatures and tested for phosphate removal from aqueous solution. The modified biochar reached its maximum phosphate adsorption capacity of 149.25 mg/g. The influence of reaction parameters on adsorption was also investigated, including temperature, solution pH, phosphate concentration, and coexisting anions. Ci et al. [39] used corn biochar with impregnated magnesium for phosphate adsorption. The biochar was pyrolyzed at 300, 450, and 600°C and dipped in $MgCl_2$ and pyrolyzed again under same conditions. The maximum phosphate adsorption using the Langmuir-Freundlich model is 239 mg/g.

The biochar produced from anaerobic digested sugar beet tailing has been studied as a phosphate adsorbent from wastewater. Yao et al. [1] indicated that MgO particles present on the biochar surface allow better phosphate ion adsorption of 133.08 mg/g according to the Langmuir model. However, the anaerobic digestion of biochar makes it more costly as anaerobic digestion requires more time and control of the reactions.

Ningyuan et al. [13] prepared a wheat straw biochar impregnated with Bismuth at 400, 500, and 600°C for application in wastewater. The bismuth impregnation increased the specific surface area and micropores which played the role of adsorption sites for phosphorus. Bismuth biochars showed high phosphate sorption ability to phosphate with maximum P adsorption capacity of 125.40 mg/g. Hui et al. [17] prepared a hydrochar composite by hydrothermal carbonization of tobacco stalk. The hydrochar composite was prepared by adding the prepared feedstock to metal solution containing AlCl3 and MgCl2 and then putting the solution in autoclave at 180°C for 12 h. However, the highest P adsorption observed is 41.16 mg P/g at 45°C

adsorption reaction time. Ming et al. [40] produced a biochar composite material which linked biochar with AlOOH nanoparticles. The biochar was produced through a slow pyrolysis of $AlCl_3^-$ pretreated biomass at 600°C. The characterization of the AlOOH biochar showed a uniform presence of AlOOH particles on biochar surface according to scanning electron microscope (SEM) studies. The Langmuir maximum capacity best describes phosphate adsorption isotherm data to be around 135 mg/g. This makes the biochar/AlOOH nanocomposite a very competitive and efficient adsorbent that can be used in the recovery of phosphate from polluted water.

Jung et al. [41] used a dried microalga as a feedstock to prepare a Mg-Al-assembled biochar. The biochar was prepared using an electro-assisted modification method by dipping the microalgae in $MgCl_2$ solution with $MgCl_2$ acting as an electrolyte. The solution pH was adjusted to 3 using NaOH solutions and 0.5 M H_2SO_4, and a current density was applied to the solid sample that was pyrolyzed at 600°C for 1 h at 5°C/min rate. This method reported the highest adsorption capacity of 887 mg/g according to the Langmuir-Freundlich model. Same authors [42] used the same electrochemical modification with changes in parameters such as using MgO nanocomposites instead of Mg-Al [41], resulting in a maximum adsorption capacity of 620 mg P/g.

5. Factors impacting phosphate adsorption

5.1 Influence of temperature

Liu et al. prepared a modified biochar using anaerobic digestion residue by chemical co-precipitation of Mg^{2+}/Fe^{3+}. Pyrolysis was performed at temperatures 500, 600, 700, and 800°C. **Figure 4** shows the effect of pyrolysis temperature on phosphate adsorption capacity. The maximum adsorption capacity on modified biochar is achieved at 600°C and adsorption decreases at 700 and 800°C. This could be explained by the disintegration of the carbon skeleton, the drop in functional groups, and reduction in surface area. It could also be explained by the pores' blockage due to their softening, carbonization, and melting during high pyrolysis temperatures [43].

On the other hand, there is no clear impact of the change of temperature on phosphate adsorption from wastewater. **Figure 5** shows no clear trend on phosphate adsorption with increasing hydrochar temperature for different tested feedstocks (W wood, D digested, and M *Miscanthus*).

5.2 Influence of pH

The influence of pH changes on P adsorption from aqueous solutions and wastewaters varies slightly between studies. Ci et al. [39] used magnesium-modified corn biochar for phosphorus removal from swine wastewater. Their study investigated the impact of initial solution pH on phosphate adsorption. **Figure 6(a)** shows that Mg-impregnated biochar adsorption increases as pH increases from 6 to 10. The adsorption reached its maximum at pH 9 and then dropped at 10. The non-modified biochar is not significantly impacted by the change in pH as it increases from 6 to 10, aside from a slight decrease in phosphate adsorption starting at pH 9. The non-modified biochar adsorption capability relied on the physical structure including the surface area, distribution and quantity of mesoporous structures, and organic functional groups. However,

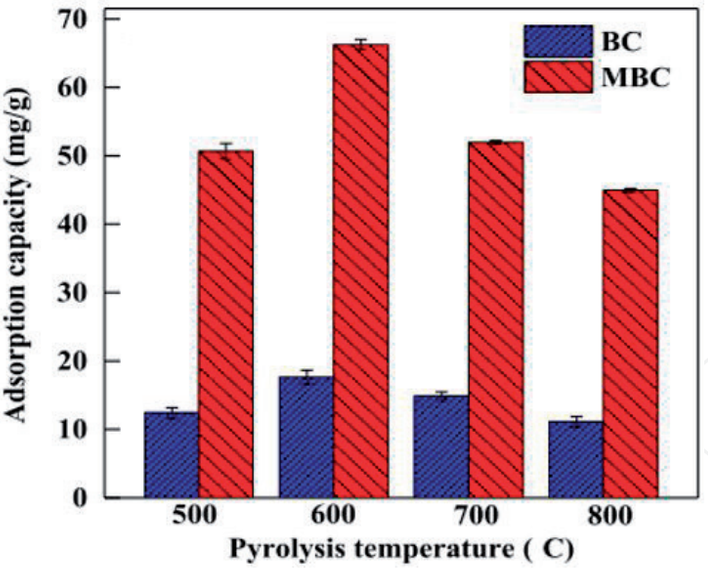

Figure 4.
The pyrolysis temperature influence on P adsorption on biochar and Mg/biochar [9].

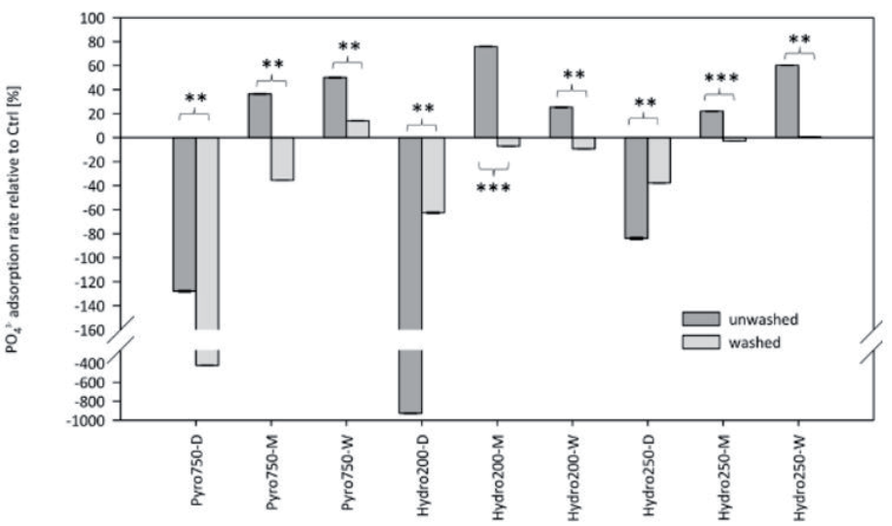

Figure 5.
The pyrolysis temperature influence on P adsorption on pyrochar and hydrochar adsorption [44].

Mg-modified biochar adsorption relies on both chemical and physical properties. P is considered as a ternary acid with the following ionization constants 2.15, 7.20, and 12.33. At an acidic solution environment (pH < 6), there is a low interaction between Mg biochar and P. $H_2PO_4^-$ is the superior in solution form at a pH above 6 and below 7.21, while HPO_4^{2-} is the superior in solution form at a pH above 7.21 and below 9. P adsorption increased with increasing chemical action, while it can decrease as adsorption sites are used. At pH between 9 and 10, P adsorption decreases as OH- competes with PO_4^{3-} on adsorption sites. The highest P adsorption amount by Mg/biochar is 239 mg/g [39].

On the other hand, Li et al. [2] found that phosphate adsorption continuously decreased when pH moved from 3.0 to 10.9 (**Figure 6(b)**). Other authors also reported that better adsorption is favored at lower pH for some adsorbents with metal oxides [11, 45]. The properties of the biochar and phosphate species distribution can explain the negative impact of the increase in pH on phosphate adsorption. At low pH levels, biochar has a more phosphate adsorption capacity.

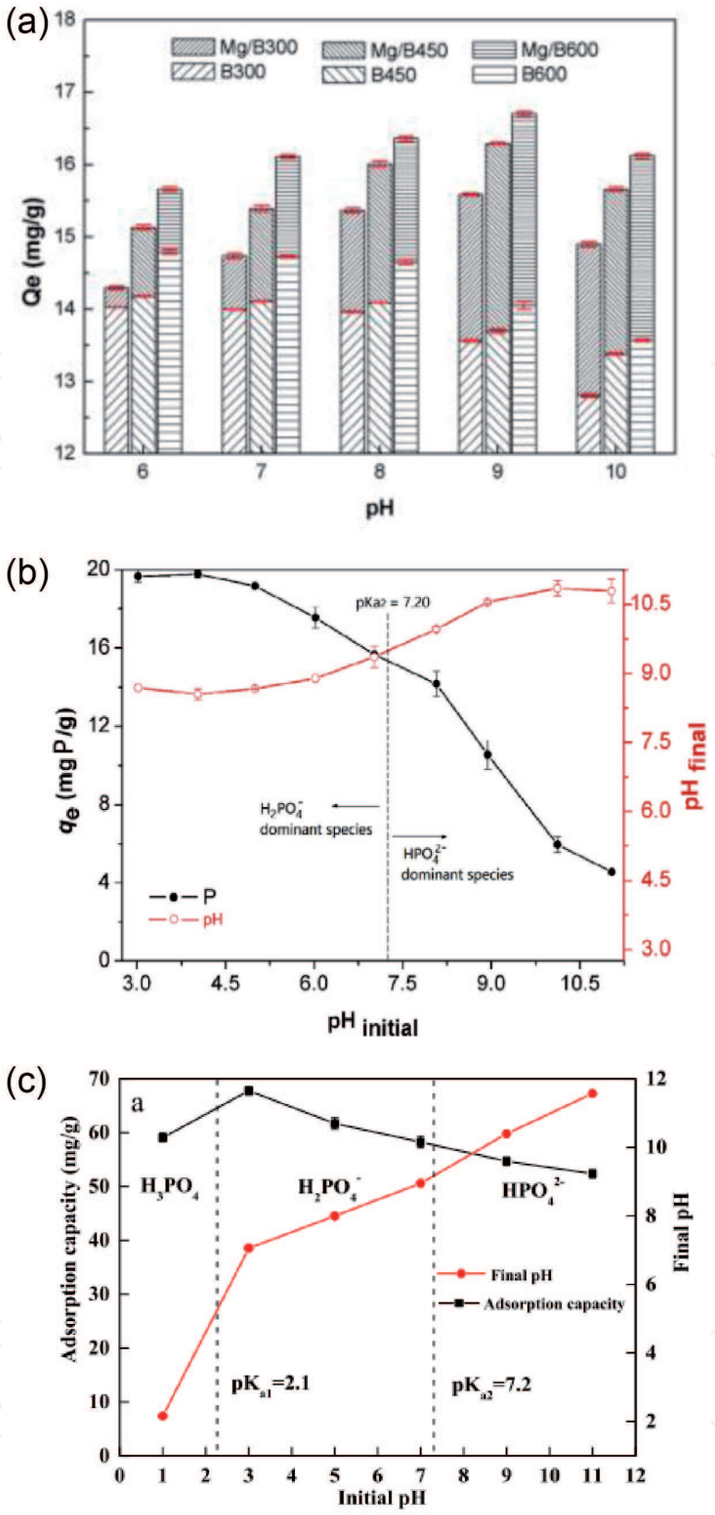

Figure 6.
The pH influence on P adsorption on biochar [2, 9, 39]. (a) effect of solution pH on the P adsorption of Mg modified corn biochar, (b) effect of solution pH on the P adsorption of Mg modified sugar cane harvest residue biochar, (c) effect of solution pH on the P adsorption of Mg modified anaerobic digestion residue biochar.

In a study by Li et al [2], phosphate existed in two forms, HPO_4^{2-} and $H_2PO_4^-$ over pH from 3 to 10.9. At lower initial pH, Mg and Fe oxides impregnated on biochar react with the solution to become $FeOH^+$ and $MgOH^+$ protons which can increase the pH of the solution. Those protons can interact with the anions HPO_4^{2-} and $H_2PO_4^-$ in an electrostatic interaction process resulting in better phosphate adsorption. The increasing pH would transform the surface to negatively charged which can cause an electrostatic repulsive interaction between phosphate anions and the

surface [46]. A similar effect was observed by Liu et al. [9] who prepared a MgO-modified biochar and studied the pH effect on phosphate adsorption. **Figure 6(c)** shows that adsorption capacity increased from pH 1 to 3 and decreased from 3 to 11. The surface property is directly related to phosphate adsorption at different pH according to Li et al. [2]. As shown in **Figure 4(c)**, phosphate exists in different forms including H_3PO_4, $H_2PO_4^-$, HPO_4^{2-}, and $H_2PO_4^-$ attached better to a MgO-modified biochar in the pH ranges because it has lower free energy which resulting in higher adsorption in the pH range 2.15–7.21.

5.3 Characteristics of adsorbed surfaces

Biochar has different components: fixed carbon, labile carbon, moisture, volatiles, and ash content. The chemical environment of the carbon in the biochar is changed during the heating process allowing the production of aromatic structures that could resist microbial decomposition. Consequently, there is a stability in biochar C compounds for long periods of time that could reach thousands of years. The biochar skeletal structure consists of different pore size minerals and carbon. Micropores control high adsorption capacity and surface area, while mesopores control liquid-solid adsorption processes and macropores are responsible for the movement of roots, hydrology, aeration, and bulk soil structure. The biochar feedstock and pyrolysis temperature are directly responsible for the pattern and pore size. SEM is used to determine the biochar pore size distribution and morphology. Biochar porous structure is composed of aromatic compounds in addition to functional groups coming from lignin biomass production. This porous structure serves as channels for the flow of nutrients in solutions such as soil solutions [47].

During pyrolysis, O and H are lost to water followed by the formation of tar-rich vapors and hydrocarbons and gases (H_2, CO, and CO_2) [48]. During pyrolysis, some inorganic compounds volatilize while the major part does not as it takes part of the biochar surface. At low temperatures, N present in biomass, Cl, and k vaporize. At high temperatures, Mg, Si, and Ca are released while Mn, S, P, and Fe are retained in biochar. At pyrolysis temperature higher than 300°C, the biochar cross section appears as graphene sheets. The graphene is described as a polyaromatic, monolayer carbon atom structure produced at temperature 250–550°C, with high breakage resistance, stability index, and electrical conductivity [49]. Aromatic C-containing groups are dominant in biochars produced at temperatures 350°C and above; these are efficient adsorbents for hazardous molecules and heavy metals. P, S, H, N, and O related to the aromatic rings control the biochar electronegativity, which has a big influence on cation exchange capacity. The biochar surface charge contributes to the biochar interaction with its environment (soil, water, organic matter) [47].

At pyrolysis above 900°C, biochar surface is deformed as walls separating adjacent pores are destructed causing a widening in the micropores. Moreover, high pyrolysis temperature decreases the amount of volatile matter in the biochar and also its particle size. This results in a higher amount of graphene layers, which leads to an increase in the solid density. Overall, biochar properties depend on parameters such as heating rate, pyrolysis temperature, furnace residence time, and type of pyrolytic reactor of feedstock. Biochar derived from animal manure has more N than plant-derived biochar. On the other hand, plant-derived biochar has a more organized pore structure and was tested as a good-quality fertilizer and good heavy metal adsorbent [50]. The biochar efficiency is impacted when fungi, bacteria, or others enter the pores. The pores get clogged and the biochar adsorption capacity decreases leading to the deactivation of biochar [47].

6. Adsorption kinetic, isotherm, and thermodynamics

6.1 Adsorption kinetics

Researchers use adsorption kinetics to study phosphate adsorption over time, in terms of solute uptake rate, considered an important characteristic defining adsorption efficiency. Solute uptake by biochar can be calculated by the difference between the initial and final quantities of the solute (phosphate) concentration in the solution (mg/L) using

$$Q = V\,(C_0 - C_f)/M \tag{4}$$

where M is the mass of the biosorbent (biochar) in g, V is the solution volume (mg/L), and C_0-C_f represents the difference between the initial and equilibrium solute concentrations (mg/L) [40, 46, 51–53].

The behavior of biochar can be examined by studying phosphate adsorption kinetics. For that, experimental kinetics are calculated using mathematical models which are listed below; all these models were tested by [54]

$$\frac{dq_t}{dt} = k_1(q_e - q_t), \text{first - order} \tag{5}$$

$$\frac{dq_t}{dt} = k_2\,(q_e - q_t)^2, \text{second - order} \tag{6}$$

$$\frac{dq_t}{dt} = k_n\,(q_e - q_t)^N, \text{N\_th - order} \tag{7}$$

$$\frac{dq_t}{dt} = \alpha \exp(-\beta q_t), \text{Elevich} \tag{8}$$

where k_1 represents the first-order, k_2 is the second-order, and k_n is Nth-order apparent adsorption rate constants in (h^{-1}, kg/mg h, and $kg^N mg^{-N} h^{-1}$). For the Elevich model, α represents the initial adsorption rate (mg/kg), and β denotes the desorption constant (mg/kg). q_e characterizes the amount of phosphate adsorbed at equilibrium, and q_t is the phosphate adsorbed at time t, in (mg/kg). First-order, second-order, and Nth-order characterize the solid solution kinetics system based on mononuclear, binuclear, and N nuclear adsorption, respectively. The Elevich model is used if the researchers would like to consider desorption in their calculations.

Krishnan et al. [11] used pseudo-second order to study phosphate adsorption on modified coir pith at different initial phosphate solution concentrations over time. **Figure 7** shows that the initial phosphate adsorption rate increases with an increase in phosphate concentration. This can be explained by the increase in covalent interactions of the adsorbent with phosphate $H_2PO_4^-$. Similar conclusions are also drawn by [55]. Zhang et al. performed kinetic studies using all the described models above and found the best fit to be the first-order model as shown in **Figure 8** [40].

6.2 Adsorption isotherms

The following isotherms are used to simulate biochar phosphate adsorption [1, 40, 46, 52, 53]:

$$q_e = \frac{KQC_e}{1 + KC_e}, \text{Langmuir} \tag{9}$$

$$q_e = K_f C_e^n \text{ Freundlich} \tag{10}$$

$$q_e = \frac{KQC_e^n}{1 + KC_e^n} \text{ Langmuir – Freundlich} \tag{11}$$

where K represents the Langmuir bonding term for energy interactions (L/mg) and K_f represents the Freundlich affinity coefficient in $mg^{(1-n)}L^n kg^{-1}$. C_e symbolizes the equilibrium solution concentration of sorbate (mg L^{-1}). Q represents the Langmuir maximum capacity (mg kg^{-1}). The Langmuir model assumes homogenous surface and monolayer adsorption on its surface without molecule interactions, while Freundlich and Langmuir-Freundlich models are empirical equations which describe the adsorption on heterogeneous equations.

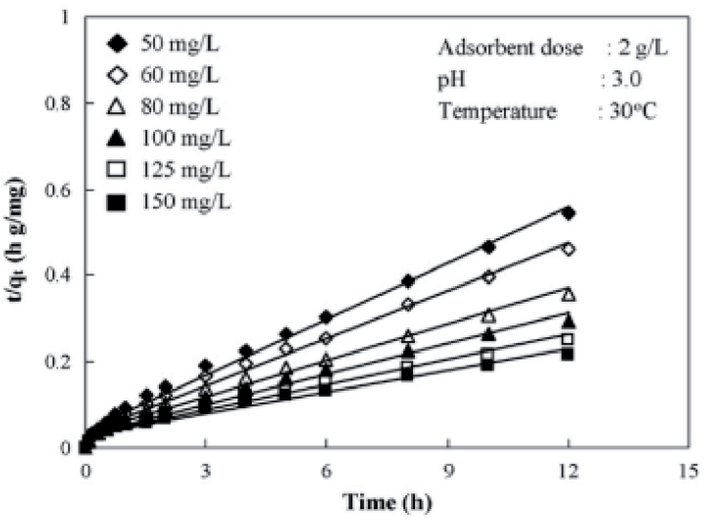

Figure 7.
Pseudo-second-order kinetic plots for phosphate adsorption on coir pith iron-modified biochar at different initial concentrations [11].

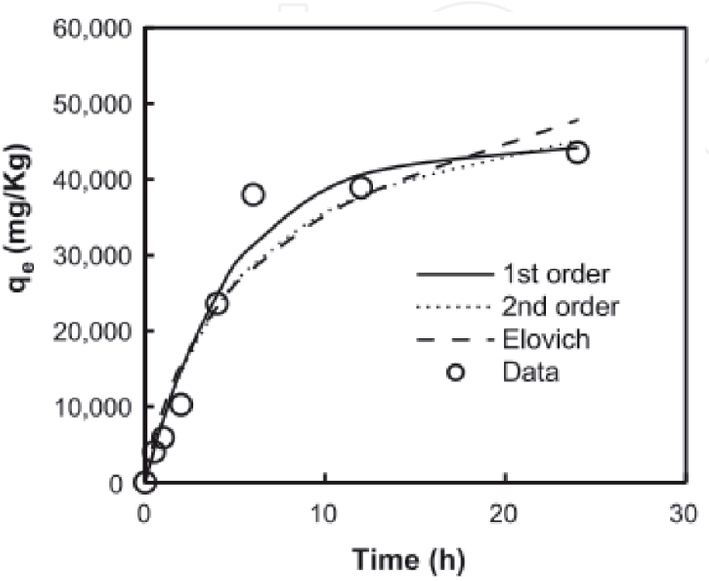

Figure 8.
Adsorption kinetic for phosphate on biochar/AlOOH nanocomposite [40].

Yao et al. [1] used these models to draw adsorption isotherm for phosphate on anaerobically digested sugar beet tailings. **Figure 9** shows that all models reproduced isotherm data correctly with correlation coefficients of 0.95. The highest adsorption capacity is presented by the Langmuir model at 133,085 mg/kg, while Freundlich and Langmuir-Freundlich models gave a better fit to the experimental data. It indicates that phosphate adsorption onto the biochar was determined by heterogeneous processes.

Zhang et al. [40] ran isotherm models of phosphate adsorption on biochar and found that both Freundlich model and Langmuir model described the isotherm data well, while the Freundlich model had a better fit for the data as shown in **Figure 10**. The maximum adsorption capacity was 135,000 mg/kg according to the Langmuir model.

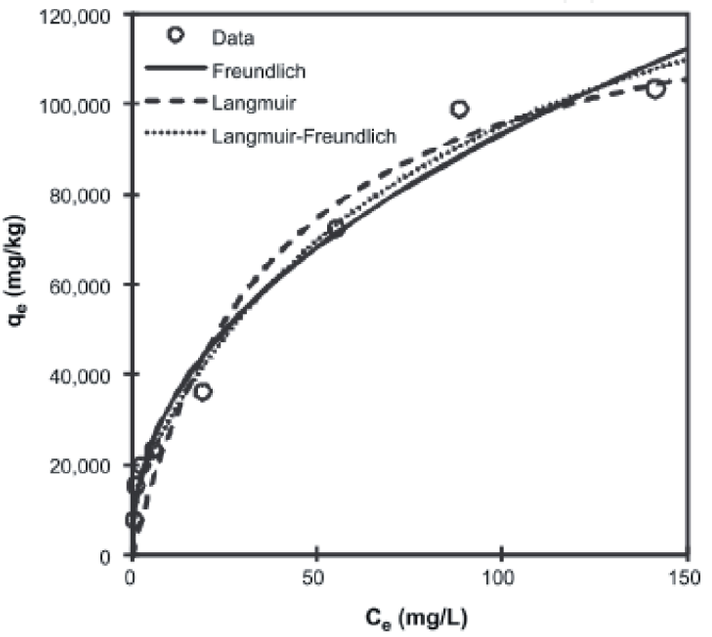

Figure 9.
Adsorption isotherm for phosphate on biochar [1].

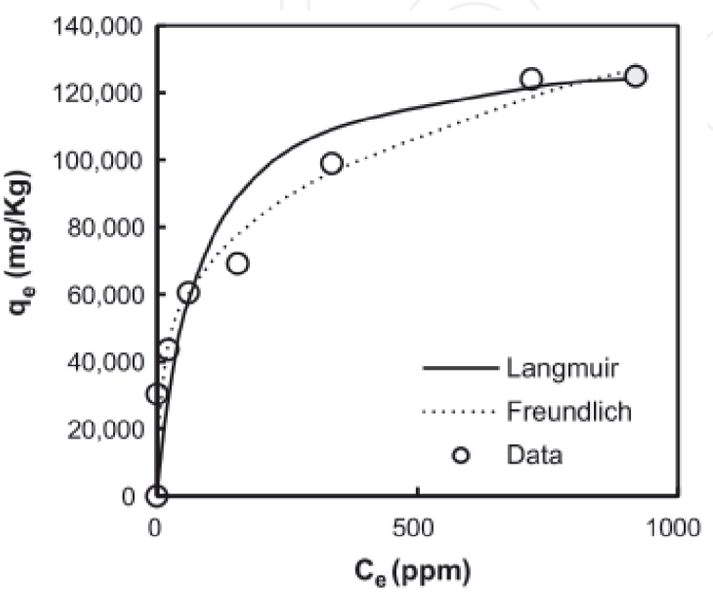

Figure 10.
Adsorption isotherm for phosphate adsorption onto biochar AlOOH nanocomposite [40].

7. Conclusion

Biomass conversion into pyrochar and hydrochar has seen a growing interest in the last years because of its use in different applications including phosphate adsorption from wastewater. Biochar has economic and sustainability benefits. In this chapter, an overview of hydrochar and pyrochar production techniques in addition to the application of biochar for phosphate adsorption from wastewater is discussed. Biochar needs to have adequate properties to be applied for phosphate adsorption from wastewater. Several factors influence the biochar properties including feedstock, pyrolysis temperature, solution pH, modification techniques, and treatment conditions. Studies have suggested that magnetic biochar has better adsorption properties than non-magnetic biochar. The biochar adsorption mechanisms are explained including ion exchange, electrostatic attraction, and chemical precipitation. Overall, biochar was proven to offer good phosphate adsorption rate along with environmental advantages such as low carbon emissions and renewability. However, further life cycle assessment studies of biochar with an evaluation of its economic benefits and environmental impacts are necessary for long-term applications.

Acknowledgements

The authors thank the USDA-CSREE-EVANS-ALLEN Project (NCX-272-5-13-130-1) for the financial support.

Author details

Aicha Slassi Sennou*, Shuangning Xiu and Abolghasem Shahbazi
Biological Engineering Program, Department of Natural Resource and Environmental Design, North Carolina A&T State University, Greensboro, North Carolina, USA

*Address all correspondence to: aslassisennou@aggies.ncat.edu

References

[1] Yao Y et al. Removal of phosphate from aqueous solution by biochar derived from anaerobically digested sugar beet tailings. Journal of Hazardous Materials. 2011;**190**(1):501-507

[2] Li R et al. Recovery of phosphate from aqueous solution by magnesium oxide decorated magnetic biochar and its potential as phosphate-based fertilizer substitute. Bioresource Technology. 2016;**215**:209-214

[3] Bensalah H et al. Removal of cationic and anionic textile dyes with Moroccan natural phosphate. Journal of Environmental Chemical Engineering. 2017;**5**(3):2189-2199

[4] Chen B, Chen Z, Lv S. A novel magnetic biochar efficiently sorbs organic pollutants and phosphate. Bioresource Technology. 2011;**102**(2):716-723

[5] Yao Y et al. Engineered carbon (biochar) prepared by direct pyrolysis of Mg-accumulated tomato tissues: Characterization and phosphate removal potential. Bioresource Technology. 2013;**138**:8-13

[6] Liu W-J et al. Mesoporous carbon stabilized MgO nanoparticles synthesized by pyrolysis of $MgCl_2$ preloaded waste biomass for highly efficient CO_2 capture. Environmental Science & Technology. 2013;**47**(16):9397-9403

[7] Arcibar-Orozco JA, Avalos-Borja M, Rangel-Mendez JR. Effect of phosphate on the particle size of ferric oxyhydroxides anchored onto activated carbon: As(V) removal from water. Environmental Science & Technology. 2012;**46**(17):9577-9583

[8] Jung K-W, Lee S, Lee YJ. Synthesis of novel magnesium ferrite ($MgFe_2O_4$)/biochar magnetic composites and its adsorption behavior for phosphate in aqueous solutions. Bioresource Technology. 2017;**245**:751-759

[9] Liu J et al. Removal of phosphate from aqueous solution using MgO-modified magnetic biochar derived from anaerobic digestion residue. Journal of Environmental Management. 2019;**250**:109438

[10] Takaya CA et al. Recovery of phosphate with chemically modified biochars. Journal of Environmental Chemical Engineering. 2016;**4**(1):1156-1165

[11] Krishnan KA, Haridas A. Removal of phosphate from aqueous solutions and sewage using natural and surface modified coir pith. Journal of Hazardous Materials. 2008;**152**(2):527-535

[12] Filippelli GM. The global phosphorus cycle. Reviews in Mineralogy and Geochemistry. 2002;**48**(1):391-425

[13] Zhu N et al. Adsorption of arsenic, phosphorus and chromium by bismuth impregnated biochar: Adsorption mechanism and depleted adsorbent utilization. Chemosphere. 2016;**164**:32-40

[14] Jiang J et al. Phosphorus removal mechanisms from domestic wastewater by membrane capacitive deionization and system optimization for enhanced phosphate removal. Process Safety and Environmental Protection. 2019;**126**:44-52

[15] Yin H et al. Phosphate removal from wastewaters by a naturally occurring, calcium-rich sepiolite. Journal of Hazardous Materials. 2011;**198**:362-369

[16] Zhang H et al. Roles of biochar in improving phosphorus availability in soils: A phosphate adsorbent and

a source of available phosphorus. Geoderma. 2016;**276**:1-6

[17] He H et al. Efficient phosphate removal from wastewater by MgAl-LDHs modified hydrochar derived from tobacco stalk. Bioresource Technology Reports. 2019;**8**:100348

[18] Kruse A, Funke A, Titirici M-M. Hydrothermal conversion of biomass to fuels and energetic materials. Current Opinion in Chemical Biology. 2013;**17**(3):515-521

[19] Wilk M, Magdziarz A. Hydrothermal carbonization, torrefaction and slow pyrolysis of Miscanthus giganteus. Energy. 2017;**140**:1292-1304

[20] Liu Z, Balasubramanian R. Upgrading of waste biomass by hydrothermal carbonization (HTC) and low temperature pyrolysis (LTP): A comparative evaluation. Applied Energy. 2014;**114**:857-864

[21] Oliveira I, Blöhse D, Ramke H-G. Hydrothermal carbonization of agricultural residues. Bioresource Technology. 2013;**142**:138-146

[22] Sabio E et al. Conversion of tomato-peel waste into solid fuel by hydrothermal carbonization: Influence of the processing variables. Waste Management. 2016;**47**:122-132

[23] Zhang Z et al. Insights into biochar and hydrochar production and applications: A review. Energy. 2019;**171**:581-598

[24] Fuch M. Literature Review of Pyrolysis Reactors. United States: Washington State Department of Ecology; 2011

[25] Liu W-J, Jiang H, Yu H-Q. Development of biochar-based functional materials: Toward a sustainable platform carbon material. Chemical Reviews. 2015;**115**(22):12251-12285

[26] Al Arni S. Comparison of slow and fast pyrolysis for converting biomass into fuel. Renewable Energy. 2018;**124**:197-201

[27] Duku MH, Gu S, Hagan EB. Biochar production potential in Ghana—A review. Renewable and Sustainable Energy Reviews. 2011;**15**(8):3539-3551

[28] Demirbas A. Effects of temperature and particle size on bio-char yield from pyrolysis of agricultural residues. Journal of Analytical and Applied Pyrolysis. 2004;**72**(2):243-248

[29] Qian K et al. Recent advances in utilization of biochar. Renewable and Sustainable Energy Reviews. 2015;**42**:1055-1064

[30] Hua M et al. Heavy metal removal from water/wastewater by nanosized metal oxides: A review. Journal of Hazardous Materials. 2012;**211-212**:317-331

[31] Loganathan P, Vigneswaran S, Kandasamy J. Enhanced removal of nitrate from water using surface modification of adsorbents – A review. Journal of Environmental Management. 2013;**131**:363-374

[32] Yin Z et al. Activated magnetic biochar by one-step synthesis: Enhanced adsorption and coadsorption for 17β-estradiol and copper. Science of the Total Environment. 2018;**639**:1530-1542

[33] Xia P et al. Struvite crystallization combined adsorption of phosphate and ammonium from aqueous solutions by mesoporous MgO-loaded diatomite. Colloids and Surfaces A: Physicochemical and Engineering Aspects. 2016;**506**:220-227

[34] Le Corre KS et al. Phosphorus recovery from wastewater by struvite

crystallization: A review. Critical Reviews in Environmental Science and Technology. 2009;**39**(6):433-477

[35] Chrispim MC, Scholz M, Nolasco MA. Phosphorus recovery from municipal wastewater treatment: Critical review of challenges and opportunities for developing countries. Journal of Environmental Management. 2019;**248**:109268

[36] Ahmed MB et al. Progress in the preparation and application of modified biochar for improved contaminant removal from water and wastewater. Bioresource Technology. 2016;**214**:836-851

[37] Welker RW. Developments in Surface Contamination and Cleaning: Detection, Characterization, and Analysis of Contaminants. Elsevier; 2012. ISBN: 978-1-4377-7883-0

[38] Bogusz A et al. Synthesis of biochar from residues after biogas production with respect to cadmium and nickel removal from wastewater. Journal of Environmental Management. 2017;**201**:268-276

[39] Fang C et al. Application of magnesium modified corn biochar for phosphorus removal and recovery from swine wastewater. International Journal of Environmental Research and Public Health. 2014;**11**(9):9217-9237

[40] Zhang M, Gao B. Removal of arsenic, methylene blue, and phosphate by biochar/AlOOH nanocomposite. Chemical Engineering Journal. 2013;**226**:286-292

[41] Jung K-W et al. Phosphate adsorption ability of biochar/Mg–Al assembled nanocomposites prepared by aluminum-electrode based electro-assisted modification method with $MgCl_2$ as electrolyte. Bioresource Technology. 2015;**198**:603-610

[42] Jung K-W, Ahn K-H. Fabrication of porosity-enhanced MgO/biochar for removal of phosphate from aqueous solution: Application of a novel combined electrochemical modification method. Bioresource Technology. 2016;**200**:1029-1032

[43] Jung K-W et al. Influence of pyrolysis temperature on characteristics and phosphate adsorption capability of biochar derived from waste-marine macroalgae (Undaria pinnatifida roots). Bioresource Technology. 2016;**200**:1024-1028

[44] Gronwald M et al. Effects of fresh and aged chars from pyrolysis and hydrothermal carbonization on nutrient sorption in agricultural soils. The Soil. 2015;**1**(1):475-489

[45] Zhang L et al. Removal of phosphate from water by activated carbon fiber loaded with lanthanum oxide. Journal of Hazardous Materials. 2011;**190**(1):848-855

[46] Ren J et al. Granulation and ferric oxides loading enable biochar derived from cotton stalk to remove phosphate from water. Bioresource Technology. 2015;**178**:119-125

[47] Qambrani NA et al. Biochar properties and eco-friendly applications for climate change mitigation, waste management, and wastewater treatment: A review. Renewable and Sustainable Energy Reviews. 2017;**79**:255-273

[48] Antal MJ, Grønli M. The art, science, and Technology of Charcoal Production. Industrial & Engineering Chemistry Research. 2003;**42**(8):1619-1640

[49] Geim AK, Novoselov KS. The rise of graphene. Nature Materials. 2007;**6**(3):183-191

[50] Uchimiya M et al. Influence of pyrolysis temperature on biochar

property and function as a heavy metal sorbent in soil. Journal of Agricultural and Food Chemistry. 2011;**59**(6):2501-2510

[51] Tafakori V et al. Equilibrium isotherm, kinetic modeling, optimization, and characterization studies of cadmium adsorption by surface-engineered *Escherichia coli*. Iranian Biomedical Journal. 2017;**21**(6):380-391

[52] Özacar M. Adsorption of phosphate from aqueous solution onto alunite. Chemosphere. 2003;**51**(4):321-327

[53] Zhang M et al. Phosphate removal ability of biochar/MgAl-LDH ultra-fine composites prepared by liquid-phase deposition. Chemosphere. 2013;**92**(8):1042-1047

[54] Gerente C et al. Application of chitosan for the removal of metals from wastewaters by adsorption-mechanisms and models review. Critical Reviews in Environmental Science and Technology. 2007;**37**(1):41-127

[55] Namasivayam C, Prathap K. Recycling Fe(III)/Cr(III) hydroxide, an industrial solid waste for the removal of phosphate from water. Journal of Hazardous Materials. 2005;**123**(1):127-134